http://dx.doi.org/10.5012/bkcs.2012.33.1.189

# ZnO Nanorods Grown on $Cd_xZn_{1-x}O$ Seed Layers with Various Cd Mole Fractions

**Min Su Kim,[†] Do Yeob Kim,[‡] Kwang Gug Yim,[†] Soaram Kim,[§] Giwoong Nam,[§] Sung-O Kim,[‡] Dong-Yul Lee,[#] and Jae-Young Leem[†,§,*]**

*[†]Department of Nano Systems Engineering, Center for Nano Manufacturing, Inje University, Gimhae, Gyungnam 621-749, Korea. [*]E-mail: jyleem@inje.ac.kr*
*[‡]Holcombe Department of Electrical and Computer Engineering, Center for Optical Materials Science and Engineering Technologies, Clemson University, Clemson, South Carolina 29634, USA*
*[§]Department of Nano Engineering, Inje University, Gimhae, Gyungnam 621-749, Korea*
*[#]Epi R&D Team, Samsung LED Co. Ltd., Suwon, Gyeonggi-do 443-373, Korea*
*Received September 15, 2011, Accepted November 15, 2011*

ZnO nanorods were grown on the $Cd_xZn_{1-x}O$ seed layers with various Cd mole fractions by hydrothermal method. The effects of the Cd mole fraction for $Cd_xZn_{1-x}O$ seed layers on the structural and optical properties of the ZnO nanorods were investigated by scanning electron microscopy, X-ray diffraction, and photoluminescence. The narrowest full-width at half-maximum and largest grain size of the $Cd_xZn_{1-x}O$ seed layers, indicating improvement in crystal quality, were observed at the Cd mole fraction of 0.5. At the Cd mole fraction of 0.5, the largest enhancement in the density, the crystal quality, and the growth rate of the ZnO nanorods was observed while their appearance was not affected significantly by the incorporation of the Cd in the $Cd_xZn_{1-x}O$ seed layers. Consequently, the luminescent properties of the ZnO nanorods were enhanced. The largest improvement in the structural and optical properties of the ZnO nanorods was observed at the Cd mole fraction of 0.5.

**Key Words :** Zinc oxide, Cadmium zinc oxide, Nanorod, Hydrothermal, Photoluminescence

## Introduction

1-D structures, such as nanowires, nanorods, and nanotubes, have aroused remarkable attention due to a great deal of potential applications in data storage, advanced catalyst, and optoelectronic devices.[1,2] As an important optoelectronic material, 1-D ZnO nanostructures also attracted extensive interest in the past decade. Especially, UV-nanowire laser under optical excitation in ZnO was realized at room temperature (RT) by Yang *et al*. in 2001.[3] Therefore, fabricating suitable nanostructures becomes more important, and will offer a base for further building nanodevices. Many different growth methods have been employed in the preparation of ZnO nanostructures. Among them, hydrothermal growth appears as the most promising method because of the low dislocation density and its cost effectiveness compared to other growth methods.[4] A metal catalyst, Au, is frequently chosen in the producing process.[5] However, a metal catalyst commonly induces extra defects in the ZnO crystals. To solve this problem, homogeneous ZnO thin layers have been widely used as seed layers.[6] The crystallinity of the ZnO nanostructures is greatly affected by crystal quality and surface morphology of seed layers.

CdO is conducting and transparent in the visible region with a direct band gap of 2.5 eV. Much more attention has been paid to the study of the electrical and optical properties of CdO films, and therefore they are useful for various applications, such as solar cells, gas sensors, low-emissivity windows, wear resistant applications, flat panel displays, and thin film resistors.[7] Moreover, the incorporation of Cd into ZnO is very useful for tuning the structural and optical properties, and surface morphology. In this work, $Cd_xZn_{1-x}O$ seed layers with different Cd content were deposited on Si substrates not only to facilitate the nucleation of ZnO nuclei but also to decrease the lattice mismatch between the Si substrate and the ZnO. The effects of the Cd mole fraction for $Cd_xZn_{1-x}O$ seed layers on the properties of the ZnO nanorods were investigated.

## Experimental Procedure

The $Cd_xZn_{1-x}O$ seed layers were grown on Si (100) substrates by sol-gel spin-coating method. The precursor solution was prepared by dissolving 0.5 M zinc acetate dihydrate [$Zn(CH_3COO)_2{\cdot}2H_2O$] in 0.5 M 2-methoxyethanol [$CH_3OCH_2CH_2OH$] as a solvent, and monoethanolamine (MEA) was added to the stable sol solution. The Cd mole fraction was controlled by the change in the cadmium acetate dihydrate [$Cd(CH_3COO)_2{\cdot}2H_2O$] to zinc acetate dihydrate. The sol solution was spin-coated onto Si substrate, rotated at 3000 rpm for 20 s. The $Cd_xZn_{1-x}O$ seed layers were heated at 300 °C for 10 min to evaporate the solvent and remove the organic residuals (named as pre-heat treatment). After the pre-heat treatment, the $Cd_xZn_{1-x}O$ thin films were cooled to RT. The spin-coating and pre-heating processes were repeated three times. In order to crystallize, the $Cd_xZn_{1-x}O$ seed layers were heated in a furnace under an air atmosphere at 550 °C for 1 h (named as post-heat

treatment). An aqueous solution of zinc nitrate hexahydrate [$Zn(NO_3)_2 \cdot 6H_2O$] and hexamethylenetetramine (HMT) [$C_6H_{12}N_4$] was prepared for hydrothermal growth of the ZnO nanorods. The growth temperature was kept constant at 140 °C for 6 h. The effects of the Cd mole fraction for $Cd_xZn_{1-x}O$ seed layers on the properties of the ZnO nanorods were investigated by scanning electron microscopy (SEM), X-ray diffraction (XRD), and photoluminescence (PL).

## Results and Discussion

Figure 1 shows SEM images of the $Cd_xZn_{1-x}O$ seed layers with various Cd mole fractions. The ZnO seed layers ($x = 0$) exhibit a rough surface with the three-dimensional (3D) island growth. The grain size and the number of voids were decreased with the increase in the Cd mole fraction. However, the grain size was rapidly increased at the Cd mole fraction of 0.75. By further increase in the Cd mole fraction ($x = 1$), the voids were dramatically formed on the surface of the seed layers.

Figure 2 shows XRD patterns of the $Cd_xZn_{1-x}O$ seed layers with various Cd mole fractions. Seven diffraction peaks at 31°, 34°, 36°, 47°, 56°, 63°, and 68° were observed from the ZnO seed layers ($x = 0$), corresponding to ZnO (100), ZnO (002), ZnO (101), ZnO (102), ZnO (110), ZnO (103), and ZnO (112), respectively. At the Cd mole fraction of 0.25, the diffraction peaks at 32° and 33° were also observed, which correspond to CdO (111) and Cd (104), respectively. The CdO (111) diffraction peak implies that the coexistence of the wurtzite structured ZnO and the rock-salt structured CdO. The Cd (104) diffraction peak is attributed to a little non-oxidized Cd.[8] The Cd (104) diffraction peak was observed from the $Cd_xZn_{1-x}O$ seed layers ($0.25 \le x \le 0.75$), which might be due to the difference in structure of the ZnO and CdO. The radius of the $Zn^{2+}$ (0.60 Å) and $Cd^{2+}$ (0.74 Å) ions is similar, but the ZnO and CdO stay in unstable condition due to the difference in structure. To relieve the unstable condition, the Cd was not fully oxidized to the rock-salt structured CdO, and a tiny amount of Cd remains a hexagonal structure.[9] As the Cd mole fraction was increased to 0.5, the intensity of the ZnO (002), CdO (220), and CdO (200) diffraction peaks was dramatically increased while that of the ZnO (101), ZnO (102), ZnO (110), ZnO (103), and ZnO (112) diffraction peaks was decreased. In addition, the CdO (220) and CdO (311) diffraction peaks appeared suddenly. These results indicate that both the wurtzite structured ZnO and rock-salt structured CdO were easily formed at the Cd mole fraction of 0.5. By further increase in the Cd mole fraction ($x \ge 0.75$), the intensity of the ZnO (002) diffraction peak was decreased while that of the Cd (220), Cd (311), and CdO (222) was increased. As the Cd mole fraction was increased to 0.5, the intensity of the ZnO (002) diffraction peaks was gradually increased and their full width at half maximum (FWHM) was decreased from 0.092° to 0.088°. A higher intensity and a narrower FWHM of the ZnO (002) diffraction peak indicate enhanced crystal quality.[10] The $Cd_xZn_{1-x}O$ seed layers with the Cd mole fraction of 0.5 was optimum condition for getting high-quality CdZnO seed layers grown on Si (100) substrates by sol-gel spin-coating method. Choi *et al.*[11] reported firstly the study on CdZnO thin films prepared by sol-gel process. Their XRD data exhibit the higher intensity of the ZnO diffraction peak by the incorporation of Cd although there is discrepancy in the value of the optimum Cd mole fraction.

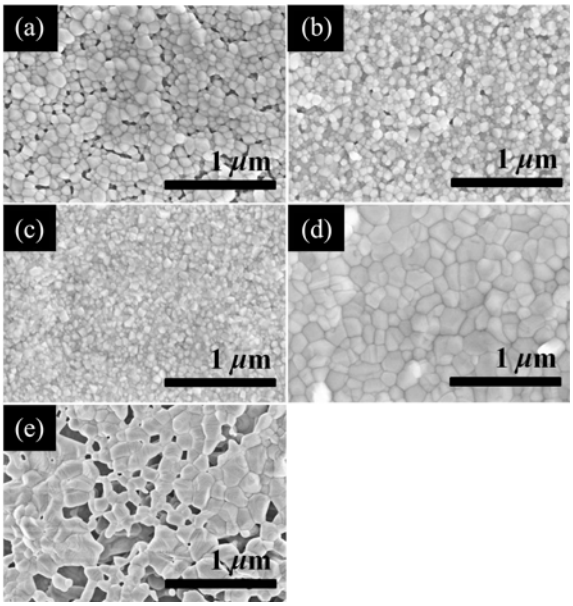


**Figure 1.** SEM images of the $Cd_xZn_{1-x}O$ seed layers with various Cd mole fractions; (a) 0, (b) 0.25, (c) 0.5, (d) 0.75, and (e) 1.

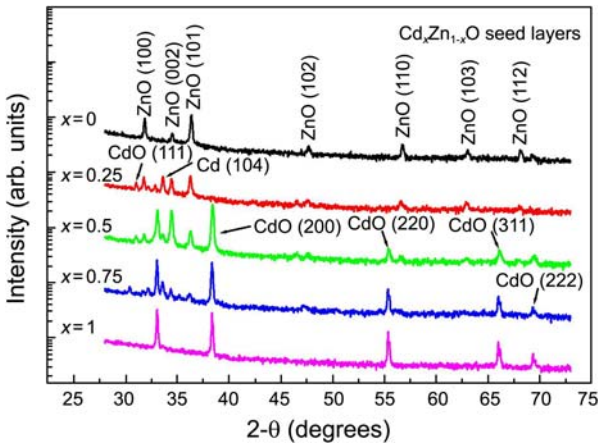


**Figure 2.** XRD patterns of the $Cd_xZn_{1-x}O$ seed layers with various Cd mole fractions.

Figure 3 shows SEM images of the ZnO nanorods grown on the $Cd_xZn_{1-x}O$ seed layers with various Cd mole fractions. The diameters of the ZnO nanorods are scattered in the range of 100 to 600 nm. The appearance of the ZnO nanorods was not significantly changed with the increase in the Cd mole fraction of the $Cd_xZn_{1-x}O$ seed layers. However, the density and the array (perpendicular to the Si substrate) of the ZnO nanorods were affected by the Cd mole fraction. The density and crystal quality of the $Cd_xZn_{1-x}O$ seed layers were enhanced as the Cd mole fraction was increased to 0.5, and consequently, the density of the ZnO nanorods was

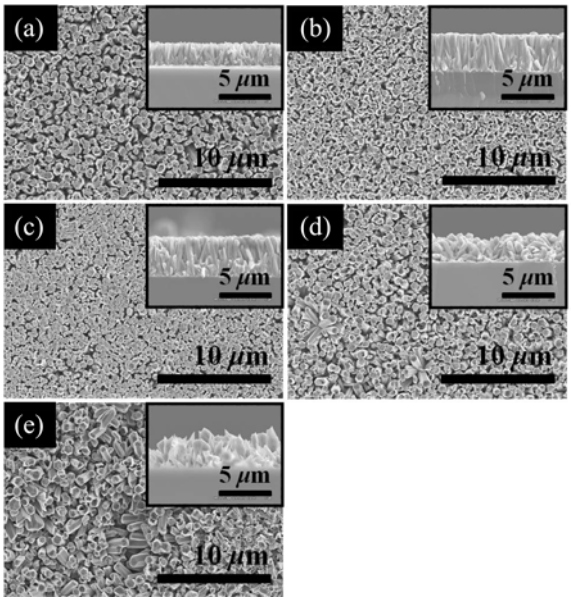


**Figure 3.** SEM images of the ZnO nanorods grown on the $Cd_xZn_{1-x}O$ seed layers with various Cd mole fractions; (a) 0, (b) 0.25, (c) 0.5, (d) 0.75, and (e) 1. The inset shows cross-sectional SEM images of the ZnO nanorods grown on the $Cd_xZn_{1-x}O$ seed layers with various Cd mole fractions.

increased. With further increase in the Cd mole fraction, the array of the ZnO nanorods was collapsed with decrease in the density. The inset shows cross-sectional SEM images of the ZnO nanorods grown on the $Cd_xZn_{1-x}O$ seed layers with various Cd mole fractions. The average length of the ZnO nanorods grown on the ZnO seed layers ($x$ = 0) was 2.3 $\mu$m. The average length of the ZnO nanorods grown on the $Cd_xZn_{1-x}O$ seed layers was increased to 3.8 $\mu$m with increasing the Cd mole fraction to 0.5. However, the average length of the ZnO nanorods was decreased by further increasing the Cd mole fraction. These results implied that the growth rate of the ZnO nanorods was affected by the Cd mole fraction of the $Cd_xZn_{1-x}O$ seed layers, which was due to enhancement of the crystal quality of the $Cd_xZn_{1-x}O$ seed layers as shown in Figure 2.

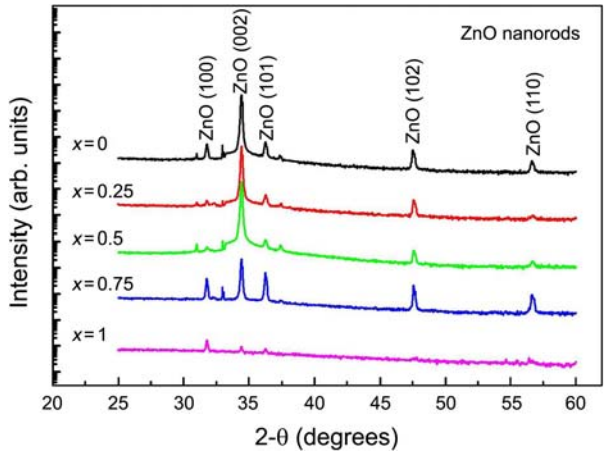


**Figure 4.** XRD patterns of the ZnO nanorods grown on the $Cd_xZn_{1-x}O$ seed layers with various Cd mole fractions.

Figure 4 shows XRD patterns of the ZnO nanorods grown on the $Cd_xZn_{1-x}O$ seed layers with various Cd mole fractions. Five ZnO diffraction peaks, 31°, 34°, 36°, 47°, and 56°, are observed. In order to describe the preferred orientation, the texture coefficient ($TC_{(hkl)}$) was calculated using the following equation:[12]

$$TC_{(hkl)} = \frac{I_{(hkl)}/I_{0(hkl)}}{1/N\Sigma_N I_{(hkl)}/I_{0(hkl)}} \quad (1)$$

where $N$ is the number of diffraction peaks and $I_{(hkl)}$ and $I_{0(hkl)}$ are the integrated intensities corresponding to the ($hkl$) reflection of the ZnO nanorods containing textured and randomly oriented crystallites. It is clear from the definition that the deviation of $TC$ from unity implies that the ZnO nanorods grow well with a preferred orientation along that diffraction plane. As shown in the inset of Figure 5(a), the values of $TC_{(100)}$, $TC_{(002)}$, $TC_{(101)}$, $TC_{(102)}$, and $TC_{(110)}$ for the ZnO nanorods grown on the ZnO seed layers ($x$ = 0) were 1.6, 94.1, 1.2, 2.4, and 0.7, respectively. The value of $TC_{(002)}$ was gradually increased as the Cd mole fraction was increased to 0.5. This indicates that the ZnO nanorods were grown with $c$-axis preferred orientation, which is because the (001) basal plane of ZnO has the lowest surface energy.[13] However, the value of the $TC_{(002)}$ was dramatically decreased by further increase in the Cd mole fraction. It is well-known that the FWHM of the ZnO (002) diffraction peak is closely related to both grain size and crystal quality.[14] The FWHM is correlated with the average grain size ($D$) of the

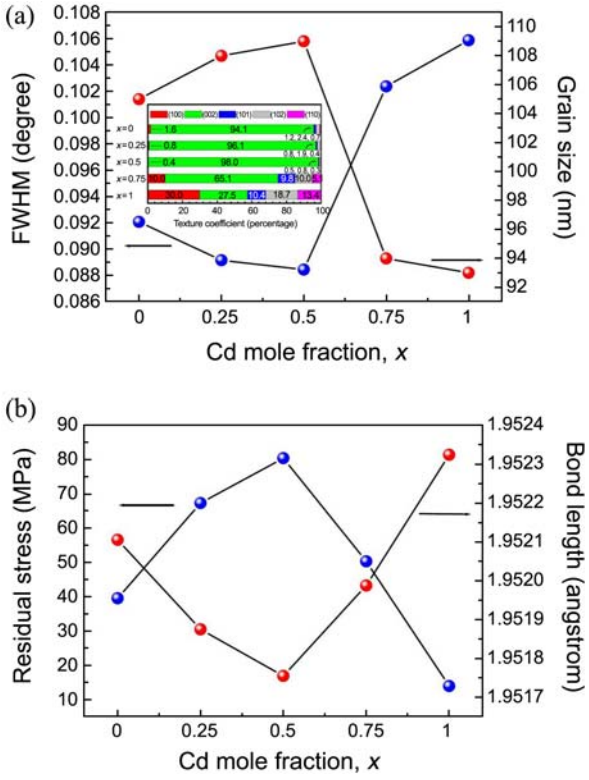


**Figure 5.** The (a) FWHM and grain size and (b) residual stress and bond length of the Zn-O in the ZnO nanorods as a function of the Cd mole fraction. The inset shows texture coefficient of the ZnO nanorods as a function of the Cd mole fraction.

ZnO nanorods by the following Scherrer's equation[15]

$$D = \frac{0.9\lambda}{\beta \cos\theta} \quad (2)$$

where $\lambda$, $\theta$, and $\beta$ are the X-ray wavelength, Bragg diffraction angle, and FWHM in radians, respectively. Figure 5(a) shows the FWHM and grain size as a function of the Cd mole fraction. The grain size was gradually increased as the Cd mole fraction was increased to 0.5, which demonstrates that the crystal quality of the ZnO nanorods was enhanced by the incorporation of the Cd in the seed layers. However, by further increase in the Cd mole fraction, the grain size was rapidly decreased. As shown in Figure 5(b), the residual stress in the ZnO nanorods was decreased with the increase in the Cd mole fraction to 0.5. However, the residual stress was increased by further increase in the Cd mole fraction, which was due to the change in the bond length of the Zn-O in the ZnO nanorods.[16] The bond length $L$ of Zn-O is given by

$$L = \sqrt{\left(\frac{a^2}{3} + \left(\frac{1}{2} - u\right)^2 c^2\right)} \quad (3)$$

where $u$ is given by (in the wurtzite structure)

$$u = \frac{a^2}{3c^2} + 0.25 \quad (4)$$

and is related to the $a/c$ ratio (ratio of lattice constant between $a$- and $c$-axis).

Figure 6 shows PL spectra of the ZnO nanorods grown on the $Cd_xZn_{1-x}O$ seed layers with various Cd mole fractions. In the UV range, a near-band-edge emission (NBE) is generated by the free-exciton (FX) recombination in the ZnO nanorods, but in the visible range, a deep-level emission (DLE) is caused by impurities and structural defects. The green emission at 2.2 eV has been attributed to various types of defects such as oxygen vacancies ($V_O$),[17] zinc vacancies ($V_{Zn}$),[18] oxygen atoms at the zinc position in the crystal lattice ($O_{Zn}$),[19] and donor-acceptor pair (DAP).[20] However, the origin is still controversial. The inset shows the FWHM and energy of the NBE peak as a function of the Cd mole fraction. The relations between the luminescence properties and crystal quality of ZnO crystals can be discussed by the PL FWHM.[21] In addition, the density of the ZnO crystals affects the luminescent efficiency.[22] Therefore, a narrower NBE peak is regarded as a clear evidence for the improvement of crystal quality. The FWHM of the NBE peak was decreased as the Cd mole fraction was increased to 0.5, indicating the enhancement of the crystal quality. It is in good agreement with the XRD results. The FWHM of the ZnO (002) diffraction and NBE peak was decreased with increasing the Cd mole fraction to 0.5. However, by further increasing the Cd mole fraction, the FWHM was increased again, which was because the CdO with cubic rocksalt structure was increased while the ZnO with hexagonal wurtzite structure was dramatically decreased as shown in Figure 2. A higher intensity and a narrower FWHM of the ZnO (002) diffraction peaks was observed at the Cd mole fraction of 0.5, which was optimum condition for getting high-quality CdZnO seed layers grown on Si (100) substrates by sol-gel spin-coating method. However, the crystal quality of the $Cd_xZn_{1-x}O$ seed layers was degraded by the excessive existence of cubic rocksalt structured CdO. The energy of the NBE peak was blue-shifted as the Cd mole fraction was increased to 0.5 owing to increase in the residual stress. On the other hand, at the Cd mole fraction above 0.75, the NBE peak was red-shifted due to the relaxation of the residual stress as shown in Figure 5(b). Kappertz *et al.*[23] suggested that the stress in ZnO films was affected by the stress relaxation and deposition parameters.

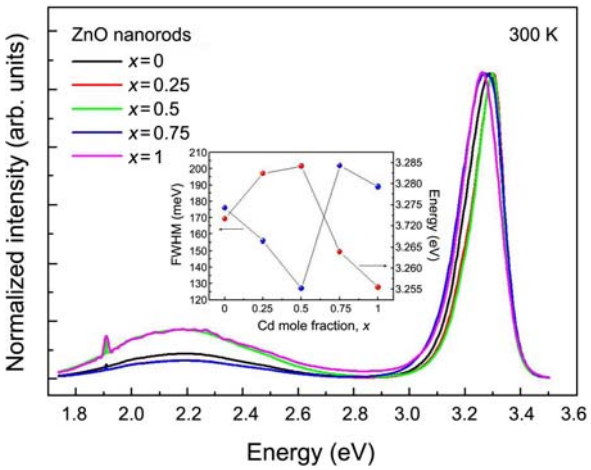


**Figure 6.** PL spectra of the ZnO nanorods grown on the $Cd_xZn_{1-x}O$ seed layers with various Cd mole fractions. The inset shows the FWHM and energy of the NBE peak from the ZnO nanorods as a function of the Cd mole fraction.

## Conclusions

The ZnO nanorods were grown on the $Cd_xZn_{1-x}O$ seed layers with various Cd mole fractions by hydrothermal method. The narrowest FWHM and the largest grain size of the $Cd_xZn_{1-x}O$ seed layers, which indicates enhanced crystal quality, were observed at the Cd mole fraction of 0.5. The appearance of the ZnO nanorods was not significantly changed by incorporation of the Cd in the $Cd_xZn_{1-x}O$ seed layers. However, the density, the array, and the growth rate of the ZnO nanorods were affected by the Cd mole fraction. The largest improvement in the density and crystallinity of the ZnO nanorods were observed at the Cd mole fraction of 0.5. In consequence, luminescent properties of the ZnO nanorods were enhanced. The largest improvement in the structural and optical properties of the ZnO nanorods was observed at the Cd mole fraction of 0.5. So, it is suggested that the Cd mole fraction of 0.5 for the $Cd_xZn_{1-x}O$ seed layers is most suitable content to obtain high-quality ZnO nanorods with good luminescent properties.

**Acknowledgment.** This work was supported by the 2011 Inje University research grant.

## References


1. Lijima, S. *Nature* **1991**, *354*, 56.
2. Daun, X. F.; Huang, Y.; Cui, Y.; Wang, J. F.; Lieber, C. M. *Nature* **2001**, *409*, 66.
3. Huang, M.; Mao, S.; Feick, H.; Yan, H.; Wu, Y.; Kind, H.; Weber, E.; Russo, R.; Yang, P. *Science* **2001**, *292*, 1897.
4. Kim, J. A.; Kim, I. K.; Kim, T.-W.; Moon, J.-H.; Kim, J. H. *J. Nanosci. Nanotechnol.* **2008**, *8*, 5485.
5. Li, M. K.; Wang, D. Z.; Ding, S.; Ding, Y. W.; Liu, J.; Liu, Z. B. *Appl. Surf. Sci.* **2007**, *253*, 4161.
6. Tao, Y.; Fu, M.; Zhao, A.; He, D.; Wang, Y. *J. Alloy. Compd.* **2010**, *489*, 99.
7. Caglar, Y.; Caglar, M.; Ilican, S.; Ates, A. *J. Phys. D.* **2009**, *42*, 065421.
8. Zúñiga-Pérez, J.; Muñoz-Sanjosé, V.; Lorenz, M.; Benndorf, G.; Heitsch, S.; Spemann, D.; Grundmann, M. *J. Appl. Phys.* **2006**, *99*, 023514.
9. Hanawalt, J. D.; Rinn, H. W.; Frevel, L. K. *Ind. Eng. Chem. Anal. Ed.* **1938**, *10*, 457.
10. Jeong, S.-H.; Park, K.-H.; Song, H.-J. *J. Korean Phys. Soc.* **2007**, *50*, 1692.
11. Choi, Y.-S.; Lee, C.-G.; Cho, S. M. *Thin Solid Films* **1996**, *289*, 153.
12. Benhaliliba, M.; Benouis, C. E.; Aida, M. S.; Yakuphanoglu, F.; Sanchez Juarez, A. *J. Sol-Gel Sci. Technol.* **2010**, *55*, 335.
13. Vaithianathan, V.; Hishita, S.; Park, J. Y.; Kim, S. S. *J. Appl. Phys.* **2007**, *102*, 086107.
14. Kim, K. K.; Jong, J. H.; Jung, H. J.; Choi, W. K.; Park, S. J.; Song, J. H. *J. Appl. Phys.* **2000**, *87*, 3573.
15. You, J. B.; Zhang, X. W.; Fan, Y. M.; Yin, Z. G.; Gai, P. F.; Chen, N. F. *Appl. Surf. Sci.* **2009**, *255*, 5876.
16. Kim, M. S.; Yim, K. G.; Cho, M. Y.; Lee, D.-Y.; Kim, J. S.; Kim, J. S.; Son, J.-S.; Leem, J.-Y. *J. Korean Phys. Soc.* **2011**, *58*, 515.
17. Kang, H. S.; Kang, J. S.; Kim, J. W.; Lee, S. Y. *J. Appl. Phys.* **2004**, *95*, 1246.
18. Tuomisto, F.; Saarinen, K.; Look, D. C.; Farlow, G. C. *Phys. Rev. B* **2006**, *72*, 085206.
19. Cho, M. Y.; Kim, M. S.; Choi, H. Y.; Yim, K. G.; Leem, J.-Y. *Bull. Korean Chem. Soc.* **2011**, *32*, 880.
20. Guo, B.; Qiu, Z. R.; Wong, K. S. *Appl. Phys. Lett.* **2003**, *82*, 2290.
21. Jeong, S. H.; Kim, B. S.; Lee, B. T. *Appl. Phys. Lett.* **2003**, *82*, 2625.
22. Yim, K. G.; Cho, M. Y.; Jeon, S. M.; Kim, M. S.; Leem, J.-Y. *J. Korean Phys. Soc.* **2011**, *58*, 520.
23. Kappertz, O.; Drese, R.; Wuttig, M. *J. Vac. Sci. Technol. A* **2002**, *20*, 2084.